ACS OMEGA

Open Access

This article is licensed under CC-BY 4.0

http://pubs.acs.org/journal/acsodf

Article

Novel Pd(II) Rollover Complexes with Antimicrobial and Antibiofilm Activity

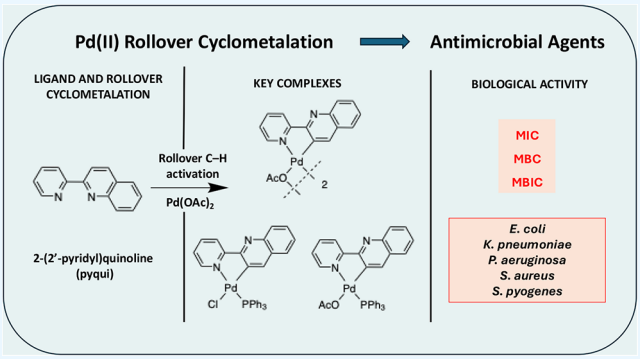
Antonio Zucca,* Bruna Canu, Giacomo Senzacqua, Sergio Stoccoro, Maria I. Pilo, Germano Orrù, Diletta Raspizzu, and Alessandra Scano*

Cite This: https://doi.org/10.1021/acsomega.6c09421

Read Online

ACCESS | Metrics & More | Article Recommendations | Supporting Information

ABSTRACT: The escalating global crisis of antimicrobial resistance (AMR) urgently demands the development of structurally diverse antimicrobial agents with novel mechanisms of action, including metal-based compounds. Herein, we report the synthesis and characterization of a series of palladium(II) complexes incorporating the 2-(2′-pyridyl)quinoline (pyqui) ligand. In addition to a simple N^N adduct [Pd(pyqui)$(OAc)_2$] (**1**), rollover cyclometalation allowed the synthesis of less-common rollover-cyclometalated dimers [Pd(pyqui-H)$(\mu\text{-OAc})]_2$ (**2**) and [Pd(pyqui-H)$(\mu\text{-Cl})]_2$ (**3**), and mononuclear rollover derivatives [Pd(pyqui-H)$(OAc)(PPh_3)$] (**4**) and [Pd(pyqui-H)$(Cl)(PPh_3)$] (**5**). The new compounds were comprehensively characterized by elemental analysis, FT-IR spectroscopy, and multinuclear (^{1}H, ^{13}C, ^{31}P) NMR spectroscopy, including two-dimensional experiments. Dynamic NMR studies revealed the coexistence of transoid and cisoid isomers in solution for the cyclometalated dimer **2**. The antimicrobial and antibiofilm properties of the complexes were evaluated against clinically relevant Gram-positive bacteria (*Staphylococcus aureus*, *Streptococcus pyogenes*), Gram-negative bacteria (*Pseudomonas aeruginosa*, *Klebsiella pneumoniae*, *Escherichia coli*), and the fungal pathogen *Candida albicans*, using agar well diffusion, minimum inhibitory concentration (MIC), minimum bactericidal concentration (MBC), and minimum biofilm inhibitory concentration (MBIC) assays. The rollover mononuclear complexes **4** and **5** were the most active compounds, exhibiting broad-spectrum antibacterial activity together with significant antibiofilm effects, particularly against Gram-positive pathogens.



INTRODUCTION

Cyclometalated complexes of noble transition metals have been extensively studied in recent years, demonstrating remarkable stability due to the chelate effect.[1,2] This inherent stability has paved the way for significant applications across diverse fields, ranging from organic synthesis and catalysis[3] to the development of innovative materials, such as sensors,[3−5] switches,[6] Light-Emitting Diodes,[7−9] and biomedicine.[10] In particular, within the biomedical field, these organometallic compounds have shown highly promising applications as both antitumoral[11−15] and antimicrobial agents.[16−19] Within this context, pyridine-based ligands constitute a family of primary importance because of their broad range of applications.[20−23]

Among the various structural motifs, rollover complexes constitute a particularly intriguing subclass of cyclometalated compounds.[24−26] These complexes originate from chelating heterocyclic ligands that, after initial coordination, undergo a unique structural rearrangement involving internal rotation and the activation of a C−H bond positioned on the opposite side of the ligand.[24,27−30] A defining feature of rollover cyclometalation is the detachment of one of the original donor atoms, typically a nitrogen atom, which remains uncoordinated. The presence of this free donor atom confers distinct, additional properties to the resulting complexes, offering new reactive sites and interaction capabilities that are usually absent in classical cyclometalated species.[24,31−33]

A rapidly developing area of application for these metal complexes is the design of novel antitumor and antimicrobial agents.[34−38] The latter has become a critical research priority due to the global health threat posed by antimicrobial resistance (AMR),[39−41] primarily driven by the indiscriminate use and abuse of conventional antibiotics over the last decades. The World Health Organization (WHO) has identified AMR as a severe crisis, compiling a list of critical priority pathogens.[42] In this scenario, noble metal complexes offer a viable alternative to classical organic drugs due to their multimodal mechanisms of action, which target multiple

Received: August 9, 2026
Revised: October 12, 2026
Accepted: November 4, 2026

ACS Publications

© XXXX The Authors. Published by American Chemical Society

Downloaded from pubs.acs.org/acsodf/article-pdf/doi/10.1021/acsomega.6c09421/6915267/acsomega.6c09421.pdf by guest on 15 November 2026

cellular components simultaneously and reduce the likelihood of resistance.[43−46] Furthermore, despite the promising activity of many metallodrugs, studies evaluating their antibiofilm activity remain relatively scarce. Biofilms provide bacteria with enhanced protection against antimicrobial agents and host immune responses, making infections extremely persistent; thus, addressing biofilm formation is a fundamental challenge in combating AMR.[47]

To address these challenges, our research group is systematically investigating a series of pyridine-based noble metal complexes to establish clear structure−activity relationships (SAR) for antimicrobial and antibiofilm efficacy.[17,18,38,48,49] In the context of this study, we turned our attention to the 2-(2′-pyridyl)quinoline ligand. Conceptually related to the classical 2,2′-bipyridine, this ligand features an extended electronic delocalization due to the condensed aromatic ring of the quinoline moiety. While 2-(2′-pyridyl)-quinoline has been previously investigated in coordination chemistry, specifically in the formation of platinum rollover complexes starting from electron-rich Pt(II) precursors,[50] its potential in biological applications has remained entirely unexplored. Furthermore, despite the well-known similarities between platinum and palladium chemistry, rollover cyclometalation with Pd(II) remains significantly rarer in the literature.[51−53]

Herein, we address this gap by reporting the synthesis and structural characterization of a novel series of palladium(II) rollover cyclometalated complexes bearing the 2-(2′-pyridyl)-quinoline ligand. By conducting a comprehensive evaluation of both their planktonic antimicrobial activity and their antibiofilm disruption capabilities, we aim to uncover valuable SAR insights. The present study not only addresses the scarcity of palladium rollover complexes but also represents the first investigation of 2-(2′-pyridyl)quinoline derivatives in a biological context, providing a new structural platform for the rational design of metal-based antimicrobials.

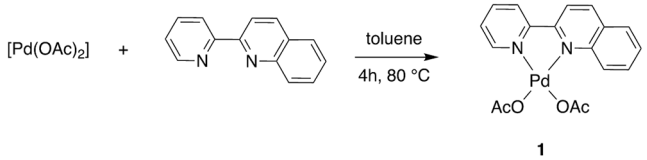
RESULTS AND DISCUSSION

Synthesis and Characterization of the Adduct [Pd(pyqui)(OAc)$_2$] (1)

The ligand 2-(2′-pyridyl)quinoline (pyqui) was synthesized in good yields by the reaction of 2-aminobenzaldehyde with 2-acetylpyridine, adapting the method reported by Al-Afyouni et al.[54]

The reaction of [Pd(OAc)$_2$] with pyqui at 80 °C in toluene afforded the adduct [Pd(pyqui)(OAc)$_2$], **1**, in high yield (90%) (Scheme 1).

Scheme 1. Synthesis of [Pd(pyqui)(OAc)$_2$], 1



1

Complex **1** is stable in air and showed no evidence of decomposition under the solution conditions employed for its spectroscopic characterization. It was extensively characterized by IR and NMR spectroscopy, specifically through 1D and 2D ^{1}H NMR. The ^{1}H NMR spectrum of **1** is consistent with the proposed formulation, which was supported by ^{1}H−^{1}H COSY and NOESY NMR experiments, allowing for the complete assignment of all proton signals. The 2D COSY analysis reveals all correlations between adjacent nuclei and notably displays two distinct signals at 2.24 and 2.14 ppm, corresponding to the two acetate groups coordinated in different, nonequivalent positions. The H^3 and H^4 protons appear as a slightly distorted AX spin system, exhibiting two doublets at 8.69 and 8.41 ppm, respectively.

The ^{1}H−^{1}H NOESY spectrum completed the signal assignment. A clear NOE effect is observed between the H$^{6'}$ nucleus (δ 8.26 ppm) and the methyl hydrogens of one of the two acetate ligands (δ 2.24 ppm), while the other acetate (δ 2.14 ppm) exhibits an NOE contact with the H^9 signal at 8.95 ppm. Additionally, a through-space interaction between the H^3 and H$^{3'}$ protons is noted, which is expected due to the N^N chelation mode (Figure 1).

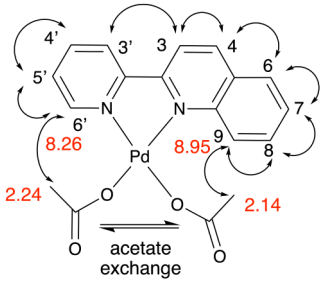


Figure 1. [Pd(pyqui)(OAc)$_2$], NOE correlations revealed by the H−H NOESY spectrum; selected proton chemical shifts are reported in red. The EXSY spectrum shows acetate exchange.

Furthermore, the EXSY portion of the 2D NOESY spectrum reveals two exchange cross-peaks between the acetate signals, demonstrating that chemical exchange between the two acetate ligands occurs on the NMR time scale. Complex **1** also exhibits concentration-dependent behavior: upon dilution with the deuterated solvent, the ^{1}H NMR spectrum shows significantly shifted signals (e.g., H$^{6'}$ δ 8.19−8.29 ppm). This behavior may arise from intermolecular interactions, such as π-π stacking, causing shielding or deshielding effects arising from the aromatic rings of neighboring complex molecules. Similar concentration-dependent effects have been previously observed in complexes bearing planar heteroaromatic ligands, such as chelated 2,2′-bipyridine, terpyridine or cyclometalated 6-phenyl-2,2′-bipyridine.[55] The ^{13}C{^{1}H} NMR spectrum (DMSO-d6) displays all 18 expected resonances. In particular, the two chemically inequivalent acetate ligands give rise to distinct methyl resonances at δ 23.37 and 23.34 ppm and carboxylate carbon resonances at δ 175.72 and 175.63 ppm.

Attempts to substitute the acetate ligands with chlorides by reacting **1** with an excess of LiCl in an H$_2$O/acetone (1:3) mixture at room temperature yielded a mixture of poorly soluble species, which were not further separated or characterized.

Synthesis of Rollover Dinuclear Complexes (2 and 3)

Cyclometalated rollover complexes of Pd(II) are less common than Pt(II) analogue.[51,52,56−58] In contrast, catalytic applications of rollover chemistry mediated by Pd(II) complexes are numerous.[24,25,56,59,60] Despite several attempts we were unable in the past to achieve Pd-rollover C−H bond activation with the simple 2,2′-bipyridine, which, at variance, was cyclo-

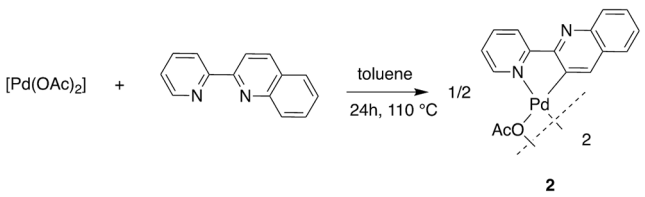
Downloaded from pubs.acs.org/acsodf/article-pdf/doi/10.1021/acsomega.6c09421/6915267/acsomega.6c09421.pdf by guest on 15 November 2026

https://doi.org/10.1021/acsomega.6c09421
ACS Omega XXXX, XXX, XXX−XXX

metalated by using the electron-rich platinum(II) precursor $[Pt(DMSO)_2Me_2]$.[61]

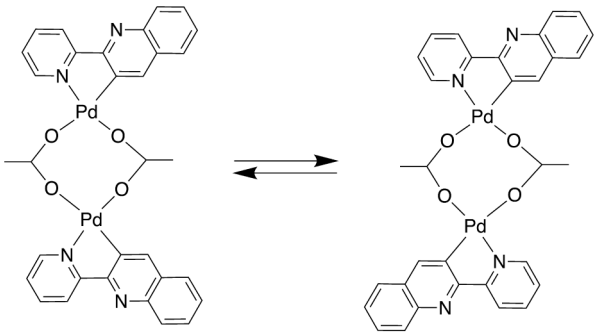
When the reaction between palladium(II) acetate and 2pyridylquinoline is performed under harsher conditions (i.e., refluxing toluene for 24 h), rollover cyclometalation occurs, leading to the isolation of the dinuclear complex $[Pd(pyqui\text{-}H)(\mu\text{-}OAc)]_2$, **2**, in good yields (Scheme 2).

Scheme 2. Synthesis of $[Pd(pyqui\text{-}H)(\mu\text{-}OAc)]_2$, 2



2

The acetate-bridged dimeric complex **2** was comprehensively characterized by IR and ^1H and ^{13}C NMR spectroscopy, including 2D H−H COSY, H−H NOESY, H−H portion of the ROESY spectrum, H−C HSQC and H−C HMBC experiments. The ^1H NMR spectrum displays two distinct sets of signals in an approximately 8:1 ratio. The rollover metalation was successful for both species as they exhibit 9 aromatic protons, as confirmed by the disappearance of the H^3 proton signal and the emergence of a singlet for the H^4 proton (at 7.41 and 7.20 ppm for the major and minor species, respectively). Both species exhibit 9 aromatic protons, in agreement with a hydrogen loss after cyclometalation. The coexistence of two species has been previously reported for similar cyclometalated dimers and was attributed to the presence of two structural isomers: *transoid* (**2t**) and *cisoid* (**2c**) (Figure 2).[62]



2c minor **2t** major

Figure 2. cisoid **2c** and transoid **2t** isomers of complex **2** with exchange in solution.

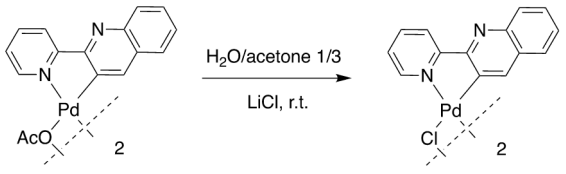
Extensive 2D NMR analysis allowed for the assignment of most of the signals and strongly support that the major species is the centrosymmetric *transoid* form (**2t**). This is sustained by the ^1H NMR spectrum showing a single peak at 2.38 ppm (integrating for 6H) for the two methyl groups of the bridging acetates. A single signal is expected for **2t**, where the methyl groups are chemically equivalent because both bridging acetates are coordinated *trans* to a $C(sp^2)$ atom on one palladium center and *trans* to a nitrogen atom on the other. Conversely, in the *cisoid* isomer (**2c**), the molecule possesses a plane of symmetry, rendering the two acetate methyls chemically inequivalent: one acetate is coordinated *trans* to carbon on both sides, while the other one is coordinated *trans* to two nitrogen atoms.

Correlation cross-peaks between the two isomers are visible in the EXSY spectrum, in line with the proposed pathway of a dynamic equilibrium in solution, likely due to detachment on one bridging acetate ligand.

In agreement with this structural assignment, the minor species in the NMR spectrum (**2c**) exhibits two distinct signals for the coordinated acetate methyls at 2.50 and 2.29 ppm (each integrating for 3H). The 2D ROESY spectrum of the major species (**2t**) shows expected spatial contacts between the bridging acetate methyls (2.38 ppm) and the adjacent $H^{6'}$ (7.89 ppm) and H^4 (7.41 ppm) protons. Finally, the ^{13}C NMR spectrum corroborates the presence of two isomers, with the bridging acetate methyl carbon of the major species resonating at 24.96 ppm.

Reaction of the **2t**/**2c** isomeric mixture with LiCl in an H_2O/acetone (1:3) mixture at room temperature allowed isolation of a new complex, which may be tentatively described as the analogous chloride-bridged dinuclear complex, $[Pd(pyqui\text{-}H)(\mu\text{-}Cl)]_2$, **3** (Scheme 3).

Scheme 3. Synthesis of $[Pd(pyqui\text{-}H)(\mu\text{-}Cl)]_2$, 3



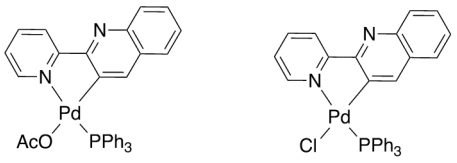
2 **3**

The ^1H NMR spectrum of **3** exhibits a series of broad signals that are generally shifted downfield compared to **2**. For instance, the $H^{6'}$ proton resonates at 8.91 ppm in **3**, compared to 7.89 ppm in the acetate-bridged precursor **2**. The broadening of the signals can be attributed to a dynamic process interconverting the *cisoid* (**3c**) and *transoid* (**3t**) forms on the NMR time scale.

Synthesis of Mononuclear Complexes (4 and 5)

Mononuclear species were successfully obtained by bridge-splitting reactions of dimers **2** and **3** with triphenylphosphine at room temperature. Starting from the **2t**/**2c** mixture, the mononuclear complex $[Pd(pyqui\text{-}H)(OAc)(PPh_3)]$, **4** (Figure 3), was isolated in quantitative yield and fully characterized.

The ^{31}P NMR spectrum of **4** features a sharp singlet at 41.42 ppm, a chemical shift compatible with a phosphorus atom coordinated *trans* to a nitrogen atom.[51] This geometry causes the signal of the $H^{6'}$ proton (8.72 ppm) to appear as a



4 **5**

Figure 3. Mononuclear rollover complexes $[Pd(pyqui\text{-}H)(PPh_3)OAc]$, **4**, and $[Pd(pyqui\text{-}H)(PPh_3)Cl]$, **5**.

Downloaded from pubs.acs.org/acsodf/article-pdf/doi/10.1021/acsomega.6c09421/6915267/acsomega.6c09421.pdf by guest on 15 November 2026

https://doi.org/10.1021/acsomega.6c09421
ACS Omega XXXX, XXX, XXX−XXX

pseudotriplet due to the combined $^{1}H-^{1}H$ and $^{1}H-^{31}P$ couplings, a feature previously observed in related systems with *trans* pyridine-triphenylphosphine coordination.[63] The chemical shift of $H^{6'}$ is not severely deshielded, likely due to the electronic effect of the *cis*-coordinated acetate ligand. In contrast, the H^{4} doublet is significantly shielded due to the anisotropic cone effect of the adjacent phenyl rings of the PPh_3 ligand. The acetate methyl group resonates at 1.45 ppm, strongly shielded due to PPh_3 proximity.

Similarly, the chloride derivative [Pd(pyqui-H)(Cl)(PPh_3)], **5**, exhibits ^{1}H, ^{13}C and ^{31}P NMR spectra consistent with the proposed structure.

The ^{31}P NMR spectrum of **5** shows a singlet at 42.46 ppm, again indicating *trans* P−N coordination, which may be compared to [Pd(N^C)(PPh_3)Cl], 43.35 ppm, (where N^C = cyclometalated 2-phenylpyridine).[64] In the ^{1}H NMR spectrum, a total of 24 aromatic protons are observed. As expected, the $H^{6'}$ proton is strongly deshielded (δ 9.76 ppm) due to the proximity of the coordinated chloride ligand. Conversely, the H^{4} proton appears as a broad doublet $^{4}J_{P-H}$ = 5.8 Hz), strongly shielded, at 7.04 ppm. The broadening of this signal indicates a likely dynamic phenomenon in solution involving the partial dissociation of the phosphine ligand. This hypothesis is confirmed by the observation that adding a slight excess of free PPh_3 collapses the signal into a singlet, due to the loss of phosphorus coupling during rapid exchange.

Complex **5** was thoroughly characterized in solution via 2D $^{1}H-^{1}H$ COSY, NOESY, HSQC, and HMBC experiments. Significant NOE effects were detected between protons $H^{6'}$/$H^{5'}$, $H^{5'}$/$H^{4'}$, $H^{6'}$/$H^{4'}$ (weak), $H^{4'}$/$H^{3'}$, H^{4}/H^{6}, and between H^{4} and the *ortho*-protons of the PPh_3 phenyl rings. The primary spatial correlations are summarized in Figure 4.

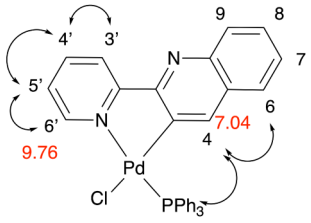


Figure 4. NOE correlations for complex **5**.

A dedicated time-dependent NMR stability study of complexes **1**, **2**, **4**, and **5** in dimethyl sulfoxide (DMSO) has been performed. The mononuclear complexes (**1**, **4**, and **5**) exhibit high stability in DMSO, as evidenced by their ^{1}H and ^{31}P NMR spectra recorded after 1 h and 5 days. These results indicate that the N^N chelate, the N^C cyclometalated framework, and the ancillary ligands remain coordinated to the metal center over the investigated period. In contrast, the ^{1}H NMR spectrum of the dinuclear complex **2** in DMSO-d_6 exhibits some signal broadening, suggesting the occurrence of a dynamic process. This behavior may be associated with partial opening of the bridging framework through coordination of DMSO to the metal center, a process that would not be unexpected given the coordinating ability of DMSO.

Antimicrobial and Antibiofilm Activity Assays

The antimicrobial activity of four synthesized complexes, **1**, **2**, **4** and **5**, was evaluated against *Escherichia coli*, *Klebsiella pneumoniae*, *Pseudomonas aeruginosa*, *Staphylococcus aureus*, *Streptococcus pyogenes*, and *Candida albicans*. The complexes were divided in two groups: in the first were evaluated the adduct **1** and the dinuclear complex **2**, then the mononuclear rollover complexes **4** and **5** were analyzed. Complex **3**, whose NMR spectrum in DMSO showed a series of large signals, indicative of the presence of more than one species and a dynamic behavior, was not tested.

A preliminary screening using the agar well diffusion assay revealed that [Pd(pyqui-H)(μ-OAc)]$_2$, **2** exhibited antibacterial activity only against *S. aureus* and *S. pyogenes*, with inhibition zones of 14 and 15 mm, respectively. In contrast, no inhibitory activity was observed against *K. pneumoniae*, *P. aeruginosa*, *E. coli*, or *C. albicans*. Conversely, [Pd(pyqui)-(OAc)$_2$], **1** did not show any detectable inhibitory effect against the tested strains, with inhibition zones of approximately 0 mm (Table 1).

Table 1. Antimicrobial Profile for [Pd(pyqui)(OAc)$_2$] 1 and [Pd(pyqui-H)(μ-OAc)]$_2$ 2 0.01 M with a Set of Gram-Positive and Gram-Negative Bacteria and Yeast[a]

	Inhibition diameter Ø mm		
	[Pd(pyqui)(OAc)$_2$], 1	[Pd(pyqui-H)(μ-OAc)]$_2$, 2	Control
Gram negative			
E. coli	–	–	Amp. 19.6 ± 0.7
K. pneumoniae	–	–	Amp. 9.5 ± 0.8
P.aeruginosa	–	–	Rif. 12.1 ± 0.5
Gram positive			
S. aureus	–	14	Ox. 22.6 ± 1.5
S. pyogenes	–	15	Amp. 23.8 ± 0.9
Yeast			
C. albicans	–	–	

[a]**Legend** – The antimicrobial activity was evaluated by measuring the inhibition zone diameter (Ø, mm). Ampicillin (Amp.), rifampicin (Rif.), and oxacillin (Ox.) were used as reference antibiotics. Control values are expressed as mean ± standard deviation.

The different outcomes of the assays (Table 2) could be attributed to steric hindrance effects within the agar matrix, which could have limited the diffusion of the tested compounds and consequently reduced their apparent activity in the agar well diffusion assay. The broth-based antimicrobial assays revealed that *E. coli*, *K. pneumoniae*, *S. aureus*, and *S. pyogenes* were susceptible to at least one of the investigated complexes. Among the tested strains, *S. aureus* showed the highest sensitivity, particularly toward [Pd(pyqui)(OAc)$_2$],**1** which displayed the lowest MIC and MBC values (6.2×10^{-4} M). Conversely, [Pd(pyqui-H)(μ-OAc)]$_2$, **2** exhibited the strongest antimicrobial activity against *S. pyogenes*, with MIC and MBC values of 3.1×10^{-4} M. Regarding antibiofilm activity, [Pd(pyqui)(OAc)$_2$], **1** was effective only against *S. pyogenes*, showing an MBIC value of 1.25×10^{-3} M, whereas [Pd(pyqui-H)(μ-OAc)]$_2$ (**2**) inhibited biofilm formation in the same strain at a lower concentration (MBIC = 3.1×10^{-4} M). No antimicrobial or antibiofilm activity was detected against *P. aeruginosa* and *C. albicans* under the experimental conditions.

These findings suggest that structural differences between the mononuclear complex **1** and the dinuclear acetate-bridged complex **2** might influence their biological behavior. Such differences may be related to factors including molecular stability, ligand exchange kinetics, cellular uptake, or

Downloaded from pubs.acs.org/acsodf/article-pdf/doi/10.1021/acsomega.6c09421/6915267/acsomega.6c09421.pdf by guest on 15 November 2026

https://doi.org/10.1021/acsomega.6c09421
ACS Omega XXXX, XXX, XXX−XXX

Table 2. Antibacterial MIC, MBC and MBIC for [Pd(pyqui)(OAc)$_2$]and [Pd(pyqui-H)(μ-OAc)]$_2$ Observed with a Set of Gram-Positive, Gram-Negative Bacteria

Strain	[Pd(pyqui)(OAc)$_2$], 1			[Pd(pyqui-H)(μ-OAc)]$_2$, 2		
	MIC mol/L	MBC mol/L	MBIC mol/L	MIC mol/L	MBC mol/L	MBIC mol/L
E. coli	2.5×10^{-3}	2.5×10^{-3}	$>1 \times 10^{-2}$	$>1 \times 10^{-2}$	$>1 \times 10^{-2}$	$>1 \times 10^{-2}$
K. pneumoniae	2.5×10^{-3}	2.5×10^{-3}	$>1 \times 10^{-2}$	$>1 \times 10^{-2}$	$>1 \times 10^{-2}$	$>1 \times 10^{-2}$
S. aureus	6.2×10^{-4}	6.2×10^{-4}	$>1 \times 10^{-2}$	$>1 \times 10^{-2}$	$>1 \times 10^{-2}$	$>1 \times 10^{-2}$
S. pyogenes	1.25×10^{-3}	1.25×10^{-3}	1.25×10^{-3}	3.1×10^{-4}	3.1×10^{-4}	3.1×10^{-4}

interactions with intracellular targets. However, given the dynamic solution behavior observed for some of the complexes, contributions from changes in speciation under the biological assay conditions cannot be excluded.

Overall, Gram-positive bacteria were more susceptible than Gram-negative species, a trend commonly reported for metal-based antimicrobial agents. The outer membrane of Gram-negative bacteria constitutes an additional permeability barrier that restricts the intracellular accumulation of coordination compounds, whereas the absence of this membrane in Gram-positive bacteria facilitates access to potential cellular targets. The lack of activity against *P. aeruginosa* may also reflect the intrinsic resistance of this microorganism, which is associated with low membrane permeability, efficient efflux pumps, and biofilm-associated defense mechanisms. The MBIC assays further highlighted the higher antibiofilm activity observed for complex **2**. Although both complexes inhibited biofilm formation by *S. pyogenes*, the dinuclear complex achieved this effect at a 4-fold lower concentration (MBIC = 3.1×10^{-4} M) than complex **1** (MBIC = 1.25×10^{-3} M).

Since biofilm formation is a major virulence factor contributing to chronic and antibiotic-resistant infections, the observed antibiofilm activity of complex **2** represents a particularly promising feature. Neither antimicrobial nor antibiofilm activity was observed against *C. albicans*, suggesting that these palladium complexes exhibit a selective antibacterial rather than antifungal profile under the experimental conditions. Taken together, these findings indicate that the investigated Pd compounds exhibit different antimicrobial and antibiofilm activity profiles under the experimental conditions employed. The acetate-bridged dinuclear complex **2** showed the most pronounced antibiofilm activity among the compounds evaluated in this group.

The second group of compounds, comprising [Pd(pyqui-H)(OAc)(PPh$_3$)],**4** and [Pd(pyqui-H)(Cl)(PPh$_3$)], **5** was evaluated against the same panel of Gram-positive and Gram-negative bacterial strains, as well as *C. albicans*, previously used for the first set of compounds. Preliminary screening using the agar well diffusion assay revealed different antimicrobial profiles among the tested compounds. Complex **4** exhibited antibacterial activity against *P. aeruginosa*, *K. pneumoniae*, and *S. aureus*, with inhibition zones of 15 mm for each strain. Complex **5** showed activity exclusively against *S. aureus*, producing an inhibition zone of 25 mm (Table 3).

The antimicrobial and antibiofilm activities of these compounds were further investigated through MIC, MBC, and MBIC assays (Table 4). The results revealed a broader activity profile compared with agar well diffusion assay, confirming that the agar diffusion method may underestimate antimicrobial efficacy due to limited diffusion of the compounds through the agar matrix.

Complex [Pd(pyqui-H)(OAc)(PPh$_3$)] (**4**) showed antibacterial activity against *K. pneumoniae*, *P. aeruginosa*, *S. aureus*, and *S. pyogenes*, with the strongest activity observed against *S. pyogenes* (MIC = 7.8×10^{-5} M; MBIC = 3.9×10^{-5} M). It was inactive against *E. coli* and *C. albicans*. Complex [Pd(pyqui-H)(PPh$_3$)(Cl)] (**5**) exhibited significant antibacterial activity against *S. aureus* and *S. pyogenes*, with the lowest MIC, MBC and MBIC values observed against *S. aureus* (7.8×10^{-5} M), while no activity was detected against *E. coli*, *K. pneumoniae*, or *C. albicans*.

Table 3. Antimicrobial Profile of [Pd(pyqui-H)(OAc)(PPh$_3$)] 4, and [Pd(pyqui-H)(Cl)(PPh$_3$)], 5 (C = 0.01 M)[a]

Strain	Inhibition diameter Ø mm		
	[Pd(pyqui-H)(OAc)(PPh$_3$)], 4	[Pd(pyqui-H)(Cl)(PPh$_3$)], 5	Control
Gram negative			
K. pneumoniae	15	–	Amp. 9.5 ± 0.8
P. aeruginosa	15	–	Rif. 12.1 ± 0.5
Gram positive			
S. aureus	15	25	Ox. 22.6 ± 1.5

[a]**Legend** – The antimicrobial activity was evaluated by measuring the inhibition zone diameter (Ø, mm). Ampicillin (Amp.), rifampicin (Rif.), and oxacillin (Ox.) were used as reference antibiotics. Control values are expressed as mean ± standard deviation.

Overall, the investigated Pd compounds exhibited distinct antibacterial and antibiofilm activity profiles under the experimental conditions employed. The differences between complexes **4** and **5** suggest that the nature of the ancillary ligand, acetate or chloride, influences their biological activity.

The individual contributions of the metal center, the phosphine ligand, and the rollover coordination framework cannot be established. However, given the stability of the complexes in DMSO, the observed activity is likely attributable to the intact complexes rather than to the free ligands or other palladium species, reflecting the combined contributions of the metal center and the coordinated ligands.

Because the compounds were initially dissolved in DMSO, diluted in microbial culture medium, and incubated for periods ranging from 24 h to several days, changes in speciation or ligand exchange during the biological assays cannot be completely excluded. Therefore, the observed activities are conservatively attributed to the tested Pd compounds under the experimental conditions rather than unequivocally to their intact molecular structures.

Comparison between the Antimicrobial Activity of Pyqui and Metal Complexes

To assess the contribution of the metal center to the biological activity of the investigated complexes, the antimicrobial and antibiofilm properties of the free ligand pyqui were also evaluated (Table 5). The results showed a limited antibacterial activity profile compared with the corresponding metal complexes. Pyqui exhibited activity against *E. coli*, *S. aureus*,

Downloaded from pubs.acs.org/acsodf/article-pdf/doi/10.1021/acsomega.6c09421/6915267/acsomega.6c09421.pdf by guest on 15 November 2026

https://doi.org/10.1021/acsomega.6c09421
ACS Omega XXXX, XXX, XXX−XXX

Table 4. Minimum Inhibitory Concentration in mol/L (MIC), Minimum Bactericidal Concentration (MBC) and Antibiofilm Assays (MBIC) Value Observed with a Set of Gram-Positive, Gram-Negative Bacteria

Strain	[Pd(pyqui-H)(OAc)(PPh_3)], 4			[Pd(pyqui-H)(PPh_3)(Cl)], 5		
	MIC mol/L	MBC mol/L	MBIC mol/L	MIC mol/L	MBC mol/L	MBIC mol/L
K. pneumoniae	3.1×10^{-4}	3.1×10^{-4}	3.1×10^{-4}	>0.01	>0.01	>0.01
P.aeruginosa	1.25×10^{-3}	1.25×10^{-3}	1.25×10^{-3}	1.25×10^{-3}	1.25×10^{-3}	1.25×10^{-3}
S. aureus	1.5×10^{-4}	1.5×10^{-4}	1.5×10^{-4}	7.8×10^{-5}	7.8×10^{-5}	7.8×10^{-5}
S. pyogenes	7.8×10^{-5}	1.5×10^{-3}	3.9×10^{-5}	7.8×10^{-5}	1.5×10^{-3}	7.8×10^{-5}

Table 5. Minimum Inhibitory Concentration in mol/L (MIC), Minimum Bactericidal Concentration (MBC) and Minimum Antibiofilm Assays (MBIC) Value Observed with a Set of Gram-Positive, Gram-Negative Bacteria

Strain	pyqui		
	MIC	MBC	MBIC
E. coli	5×10^{-3}	5×10^{-3}	5×10^{-3}
S. aureus	5×10^{-3}	5×10^{-3}	5×10^{-3}
S. pyogenes	2.5×10^{-3}	2.5×10^{-3}	2.5×10^{-3}

and *S. pyogenes*, with MIC, MBC, and MBIC values of 5×10^{-3} M, for *E. coli* and *S. aureus*, and 2.5×10^{-3} M for *S. pyogenes*. Conversely, no antimicrobial or antibiofilm activity was observed against *K. pneumoniae*, *P. aeruginosa*, or *C. albicans* at the tested concentrations (>0.01 M). The agar well diffusion assay did not reveal any inhibition zones for the free ligand pyqui against any of the tested microorganisms, indicating that it lacks detectable antimicrobial activity under the experimental conditions employed. Comparison with the free ligandindicates that some of the investigated Pd complexes exhibit enhanced antimicrobial and antibiofilm activity, as reflected by their lower MIC, MBC, and MBIC values. The different activity profiles observed among the complexes might be associated with differences in their coordination environment and may contribute to the distinct biological responses observed.

Furthermore, although the NMR spectra recorded in DMSO did not show evidence of free PPh_3 or other detectable palladium-containing species under these conditions, possible changes in speciation under the biological assay conditions cannot be excluded. Such changes may therefore need to be considered when interpreting the observed biological activity. Additional biological controls and dedicated stability and speciation studies under biologically relevant conditions would therefore be required to clarify the relationship between the coordination environment and the observed antimicrobial and antibiofilm activity.

CONCLUSIONS

This work has demonstrated the successful synthesis and characterization of a series of palladium(II) complexes incorporating the 2-(2′-pyridyl)quinoline ligand (pyqui), including, in addition to a simple coordination adduct, a series of rare cyclopalladated rollover complexes. All compounds were comprehensively characterized, in particular by means of NMR spectroscopy. Dynamic NMR studies on the acetate-bridged dimer **2** revealed the coexistence of *transoid* (major, ca. 89%) and *cisoid* (minor, ca. 11%) isomers in solution, with interconversion between the two forms confirmed by EXSY spectroscopy, most likely mediated by reversible dissociation of one bridging acetate ligand. The results demonstrate that the N^C rollover metallacycle is robust, and provides an enhanced stability to the corresponding complexes.

Four palladium(II) complexes were evaluated for their antimicrobial properties, allowing the influence of different coordination environments on their biological behavior to be assessed. The antimicrobial and antibiofilm assays demonstrated that the investigated complexes display distinct biological activity profiles under the experimental conditions employed, although the present data do not allow a definitive structure−activity relationship to be established.

Among the first series of compounds, the acetate-bridged dinuclear complex **2** exhibited higher antibacterial and antibiofilm activity against *Streptococcus pyogenes* compared with the mononuclear complex **1**, showing the lowest MIC, MBC, and MBIC values within this series. In contrast, complex **1** displayed a broader antibacterial activity profile, being active against *E. coli*, *K. pneumoniae*, *S. aureus*, and *S. pyogenes*. Notably, complex **1** showed the highest activity against *S. aureus*, whereas complex **2** exhibited greater potency specifically against *S. pyogenes*. These findings indicate that the two complexes display distinct antibacterial profiles, with complex **1** showing broader activity and complex **2** showing enhanced potency against *S. pyogenes*. These differences indicate that the two complexes exhibit distinct biological profiles under the experimental conditions employed; however, considering the dynamic solution behavior observed for complex **2**, possible contributions from changes in speciation under the biological assay conditions cannot be completely excluded. It should also be noted that complex **2** is a dinuclear species; therefore, at the same formal complex concentration, the concentration of palladium centers is twice that of the mononuclear complexes.

The mononuclear rollover cyclometalated phosphine derivatives **4** and **5** displayed high antibacterial potency, reaching MIC values in the 10^{-5} M range against Gram-positive bacteria. Complex **4** exhibited the broadest antibacterial spectrum, retaining activity against both Gram-positive and selected Gram-negative bacteria, whereas complex **5** was particularly effective against *S. aureus*. Both compounds also showed significant antibiofilm activity, although the present data do not allow the enhanced activity of these complexes to be unequivocally attributed to the introduction of the triphenylphosphine ligand.

Comparison with the free ligand clearly showed that some of the investigated Pd complexes exhibited higher antimicrobial and antibiofilm activities than pyqui under the experimental conditions employed. However, since $Pd(OAc)_2$ and free PPh_3 were not evaluated as additional controls, the individual contributions of the Pd(II) center, the phosphine ligand, and the intact coordination framework cannot be independently established

The enhanced activity observed for some of the Pd complexes may be associated with differences in their

Downloaded from pubs.acs.org/acsodf/article-pdf/doi/10.1021/acsomega.6c09421/6915267/acsomega.6c09421.pdf by guest on 15 November 2026

https://doi.org/10.1021/acsomega.6c09421
ACS Omega XXXX, XXX, XXX−XXX

coordination environments and physicochemical properties; however, the present data do not allow these effects to be assigned specifically to metal coordination, phosphine substitution, or the rollover framework. In addition, the strong *trans* influence of the metalated carbon in the robust N^C rollover scaffold may influence the lability of the acetate or chloride coligand, although the biological consequences of such processes were not directly investigated in the present study. Possible differences in cellular uptake or interactions with intracellular targets may also contribute to the observed biological profiles, but these aspects require dedicated mechanistic investigations. Overall, the investigated complexes showed selective activity toward Gram-positive bacteria, whereas Gram-negative strains and *Candida albicans* were generally less susceptible, consistent with the greater permeability barrier provided by the outer membrane of Gram-negative microorganisms. Among the investigated compounds, the rollover complexes **2**, **4**, and **5** showed pronounced antimicrobial and antibiofilm activity under the experimental conditions employed and may therefore represent interesting candidates for further biological investigation.

Taken together, these results demonstrate that the rollover cyclometalation of palladium(II) with the pyqui ligand affords a versatile coordination framework associated with distinct biological activity profiles. The differences observed among the investigated complexes provide a basis for further studies aimed at understanding the relationship between coordination environment and biological activity, although the present data do not establish a specific beneficial role for phosphine substitution or the N^C rollover coordination mode. Further investigations into the mechanism of action, cytotoxicity against human cell lines, and *in vivo* efficacy are warranted to establish the therapeutic potential of this class of compounds. Overall, this work demonstrates that rollover cyclometalation represents an interesting feature of palladium coordination chemistry that may also provide a useful framework for the exploration of biologically active metal complexes. The combination of distinct coordination environments and promising antimicrobial activity makes this family of compounds a potentially interesting platform for further investigation of palladium-based antimicrobial complexes.

EXPERIMENTAL SECTION

The ^{1}H, ^{13}C and ^{31}P NMR spectra were recorded at 400.13, 100.61, and 161.97 MHz respectively, using a Bruker Avance III 400 spectrometer, at 298 K. Data are reported in the following order: chemical shift (ppm, δ, referenced to TMS for ^{1}H and ^{13}C, and to H_3PO_4 for ^{31}P) multiplicity, corresponding nucleus/nuclei, integration, coupling constants (Hz). 2D NMR spectra (COSY, NOESY, ROESY, HMBC, and HMQC) were acquired using standard pulse sequences. The NOESY, EXSY and ROESY spectra were acquired with mixing times of 300 and 200 ms, respectively, at 298 K, c = 2×10^{-2} M.

The NMR spectra were recorded by Dr. Maria Orecchioni (Department of Medicine, Surgery and Pharmacy, UNISS). FT-IR spectra were recorded with a JASCO (Tokyo, Japan) 4600 FT/IR spectrophotometer.

Evaluation of Antimicrobial Activity

The complexes were tested against Gram-positive strains (*Staphylococcus aureus* DSM 1104 and *Streptococcus pyogenes* DSM 20565), Gram-negative strains (*Klebsiella pneumoniae* DSM 681, *Escherichia coli* DSM 1103, *Pseudomonas aeruginosa* DSM 1117) and yeast (*C. albicans* DSM 1386). Bacterial strains were obtained from the DSMZ (German Collection of Microorganisms and Cell Cultures, Germany). Antibacterial and antifungal activities were evaluated with reference to the relevant Clinical and Laboratory Standards Institute (CLSI) guidelines. The broth microdilution method was adapted from the CLSI recommendations to accommodate the physicochemical properties of the tested Pd complexes and the experimental design of this study. The main modifications concerned the preparation of the compounds as DMSO stock solutions, the initial compound concentration, the inoculum volume, and the serial dilution procedure. The modified procedure is described in detail below.

Stock solutions of the compounds were freshly prepared immediately before each experiment by dissolving the appropriate amount of each Pd complex in 1 mL of DMSO to obtain a concentration of 0.02 M.

Antimicrobial Susceptibility Testing

The preliminary antimicrobial activity of the compounds was evaluated using an agar well diffusion assay adapted from previously published procedures. Mueller−Hinton agar (25 mL; Microbiol, Uta, Cagliari, Italy), maintained at 55 °C, was poured into sterile 90 mm Petri dishes. Before solidification, sterile iron rivets (10 mm diameter, 2 mm thickness;) were placed in the agar to form wells, which were removed after solidification. A standardized bacterial suspension (5×10^{7} CFU) was evenly spread onto the agar surface using a sterile swab. A 50 μL aliquot of each test compound was dispensed into the wells. The aerobic strains were sown in Petri dishes containing Mueller Hinton Agar and Sabouraud Dextrose Agar (*C. albicans*) and incubated in air at 37 °C for 24 h, while the microaerophilic species were sown in Petri dishes containing Schaedler Agar and incubated in 5% CO_2 at 37 °C. After incubation, the diameter of the inhibition halo was measured. All experiments were performed in triplicate. The inhibition-zone diameters were considered qualitative or semi-quantitative indicators of antimicrobial activity and were not interpreted as direct measures of intrinsic antimicrobial potency. Because diffusion through agar may be influenced by the physicochemical properties of the tested compounds, MIC and MBC values obtained by broth microdilution were considered more appropriate quantitative parameters for comparing the antimicrobial activity of the tested compounds.

Minimum Inhibitory Concentration (MIC) and Minimum Bactericidal Concentration (MBC) Tests

MIC values were determined using the broth microdilution method in sterile 96-well plates.

For each microorganism, the microbial inoculum was prepared in 5 mL of the appropriate broth: Mueller-Hinton broth (MHB) for *S. aureus*, *K. pneumoniae*, *E. coli*, and *P. aeruginosa*; Schaedler broth for *S. pyogenes*; and Sabouraud broth for *C. albicans*. The inoculum was adjusted to approximately 1×10^{6} CFU/mL.

The inoculum density was assessed spectrophotometrically at 550 nm. Subsequently, 150 μL of the standardized microbial inoculum was added to each well. For each compound, 150 μL of the corresponding compound stock solution (0.02 M) was added to the first well, resulting in a final volume of 300 μL and a final compound concentration of 0.01 M.

2-fold serial dilutions were subsequently performed by transferring 150 μL from the first well into the subsequent well containing 150 μL of microbial inoculum, followed by thorough mixing. The same procedure was repeated sequentially for the subsequent wells, resulting in a 2-fold decrease in compound concentration at each dilution step. Thus, the final compound concentrations were 1×10^{-2} M, 5×10^{-3} M, 2.5×10^{-3} M, 1.25×10^{-3} M, 6.25×10^{-4} M, and so forth.

Assays were performed in triplicate. After incubation for 24−48 h at 37 °C, microbial growth was assessed by measuring the absorbance at 600 nm using a microplate photometer (Multiskan FC, Thermo Fisher Scientific, Italy) compared with the corresponding uninoculated blank control. The MIC was defined as the lowest compound concentration that prevented detectable microbial growth, After MIC determination, 50 μL aliquots from all wells showing no detectable

Downloaded from pubs.acs.org/acsodf/article-pdf/doi/10.1021/acsomega.6c09421/6915267/acsomega.6c09421.pdf by guest on 15 November 2026

https://doi.org/10.1021/acsomega.6c09421
ACS Omega XXXX, XXX, XXX−XXX

microbial growth were plated onto the corresponding solid medium and incubated at 37 °C for 24 h.

The minimum bactericidal concentration (MBC) is defined as the lowest concentration of an antimicrobial agent that kills 99.9% of the bacterial population.

Antibiofilm Assay (MBIC Determination)

Biofilm inhibitory activity was evaluated using the crystal violet staining assay to determine the minimum biofilm inhibitory concentration (MBIC), following the protocol of the University of Montana Center for Biofilm Engineering, with modifications. Briefly, bacterial strains were inoculated into 96-well polystyrene microplates containing Mueller−Hinton broth supplemented with serial dilutions of compounds. The plates were incubated at 37 °C for 5 days under static conditions to allow biofilm formation. Following incubation, the planktonic cells were carefully removed, and the wells were washed three times with sterile 0.9% NaCl solution to eliminate nonadherent cells. The remaining biofilms were stained with 100 μL of 0.1% (w/v) crystal violet for 10 min. Excess stain was removed by washing the wells with distilled water, after which the plates were air-dried at room temperature (25 °C) for 15 min. The crystal violet bound to the biofilm biomass was then solubilized with 300 μL of 30% (v/v) acetic acid, and the absorbance was measured at 550 nm using a microplate reader (SLT-Spectra II, SLT Instruments, Germany). The MBIC was defined as the lowest concentration of compound that inhibited biofilm formation, resulting in an absorbance value comparable to that of the negative control (uninoculated medium).

PREPARATIONS

Synthesis of 2-(2′-Pyridyl)quinoline

2-Aminobenzaldehyde (2.013 g, 16.5 mmol) and 2-acetylpyridine (1.85 mL, 16.5 mmol) were combined with KOH (37.0 g, 0.66 mol) in ethanol (50 mL) and heated at 85 °C for 22 h, affording a dark red suspension. The mixture was filtered, and the filtrate was evaporated to dryness under reduced pressure. The residue was taken up in CH_2Cl_2, dried over $MgSO_4$, filtered through a pad of Celite, and concentrated under reduced pressure to give a red oil/solid. The crude product was purified by column chromatography on silica gel, eluting with a mixture hexane/ethyl acetate 1:6, to afford 2-(2′-pyridyl)-quinoline as a pale solid (2.760 g, 13.4 mmol, 81%). ^{1}H NMR ($CDCl_3$) δ 8.77 (ddd, $H^{6'}$, 1H, J = 4.8 Hz, J = 1.7 Hz, J = 0.9 Hz); 8.68 (dt, $H^{3'}$, 1H, J = 8.0, Hz, J = 1.1 Hz); 8.59 (d, H^3, 1H, J = 8.7 Hz); 8.31 (d, H^4, 1H, J = 8.7, Hz); 8.20 (ddd, H^9, 1H, J = 8.6 Hz, J = 1.8 Hz, J = 0.9 Hz); 7.87−7.92 (m, H^7 and $H^{4'}$, 2H); 7.76 (ddd, H^5, 1H, J = 8.4 Hz, J = 6.9 Hz, J = 1.6 Hz); 7.58 (ddd, H^6, 1H, J = 8.1 Hz, J = 6.9 Hz, J = 1.2 Hz); 7.38 (ddd, $H^{5'}$, 1H, J = 7.5 Hz, J = 4.8 Hz, J = 1.2 Hz).

Synthesis of [Pd(pyqui)(OAc)$_2$] (1)

A mixture of [$Pd(OAc)_2$] (219.9 mg, 0.98 mmol) and pyqui (202.1 mg, 0.98 mmol) in toluene (20 mL) was stirred at 80 °C for 4 h. The resulting precipitate was collected by vacuum filtration, washed with diethyl ether, and dried under vacuum to afford the product as a yellow solid (381.4 mg, 0.88 mmol, 90%). Mp (dec.) 146−8 °C. Elemental Analysis, calculated for $C_{18}H_{16}N_2O_4Pd$: C, 50.19; H, 3.74; N, 6.50%; found: C, 50.46; H, 3.52; N, 6.61%. ^{1}H NMR ($CDCl_3$) δ 8.95 (d, H^9, 1H, J = 8.9 Hz); 8.69 (d, H^3, 1H, J = 8.6 Hz); 8.64 (d, $H^{3'}$, 1H, J = 8.1 Hz); 8.41 (d, H^4, 1H, J = 8.6 Hz); 8.26 (dd, $H^{6'}$, 1H, J = 5.8, 1.4 Hz); 7.94 (td, $H^{4'}$, 1H, J = 8.0 Hz); 7.79 (m, H^8, 1H); 7.67−7.59 (m, H^7−H^6 overlapping, 2H); 7.25 (m, $H^{5'}$, 1H); 2.24 (s, OAc, 3H); 2.14 (s, OAc, 3H). **^{1}H NMR (DMSO-d_6)** δ 8.95 (d, J = 8.6 Hz, 1H), 8.77 (d, J = 8.8 Hz, 1H), 8.73 (d, J = 7.9 Hz, 1H), 8.64 (d, J = 8.8 Hz, 1H), 8.39 (td, J = 7.9, 1.4 Hz, 1H, H4′), 8.23 (dd, J = 5.6, 1.1 Hz, 1H, H6′), 8.16−8.13 (m, 1H), 7.94−7.88 (m, 1H), 7.83−7.77 (m, 2H), 1.96 (s, 3H, CH_3 OAc), 1.80 (s, 3H, CH_3 OAc). ^{13}C{^{1}H} NMR ($CDCl_3$): δ 182.04 (COO), 162.76, 161.74, 149.08, 145.71, 141.66, 137.57, 137.41, 129.16, 128.74, 127.64, 126.56, 123.19, 121.22, 24.96 (CH_3) ppm. FT-IR, cm^{-1}: 1634 (s), 1597 (s).

Synthesis [Pd(pyqui-H)(μ-OAc)]$_2$ (2)

A mixture of [$Pd(OAc)_2$] (96.7 mg, 0.43 mmol) and pyqui (89.7 mg, 0.43 mmol) in toluene (15 mL) was stirred at 110 °C for 24 h. The resulting mixture, containing a black precipitate (palladium metal) in a brownish solution, was filtered through a pad of Celite under vacuum to remove the deposited palladium. The filtrate was concentrated under reduced pressure, and the solid residue was triturated with diethyl ether (ca. 30 min), collected by vacuum filtration, and dried under vacuum to afford the product as a yellow solid (89.7 mg, 0.12 mmol, 56%). Mp = 245−250 °C (dec). ^{1}H NMR ($CDCl_3$): the spectrum shows the presence of two species in approximately 8:1 ratio. Elemental Analysis, calculated for $C_{32}H_{24}N_4O_4Pd_2$: C, 51.84; H, 3.26; N, 7.56%). %; found: C, 51.67; H, 3.43; N, 7.44%. ^{1}H NMR. Main species (transoid): δ 7.89 (d, $H^{6'}$, 1H, J = 5.4 Hz); 7.85 (d, H^6, 1H, J = 8.4 Hz); 7.69 (d, $H^{3'}$, 1H, J = 8.0 Hz); 7.60−7.53 (m, H^7 and H^9, 2H); 7.44 (m, H^8, 1H); 7.41 (s, H^4, 1H); 7.08 (td, $H^{4'}$, 1H, J = 7.7 Hz, J = 1.5 Hz); 6.29 (m, $H^{5'}$, 1H); 2.38 (s, CH_3, 6H). Secondary species (cisoid), selected signals: δ 8.19 (d, $H^{6'}$, 1H, J = 5.4 Hz); 7.20 (s, H^4, 1H); 6.98 (m, $H^{5'}$, 1H); 2.50 (s, CH_3, 3H), 2.29 (s, CH_3, 3H). ^{13}C NMR ($CDCl_3$): main species (transoid): δ 182.02 (COO); 162.74; 161.72; 149.06 ($C^{6'}$); 145.70; 141.64; 137.56 ($C^{4'}$); 137.40; 129.14; 128.73; 127.63; 126.54; 123.18 ($C^{5'}$); 121.21 ($C^{3'}$); 24.96 (CH_3). FT-IR, cm^{-1}: 1557 (s), 1546 (s).

Synthesis of [Pd(pyqui-H)(μ-Cl)]$_2$, 3

A mixture of [Pd(pyqui-H)(μ-OAc)]$_2$ (91.0 mg, 0.12 mmol) and LiCl (250.3 mg, 5.905 mmol) in a H_2O/acetone mixture 1:3 v/v (40 mL) was stirred at room temperature for 24 h. The resulting orange suspension was collected by vacuum filtration, washed with diethyl ether, and dried under vacuum to afford the product as an orange solid (51.6 mg, 0.08 mmol, 66%). M.P. slow decomposition at T > 240 °C. ^{1}H NMR ($CDCl_3$) δ 8.91 (s, broad, $H^{6'}$, 1H); 8.38 (d, 1H, J = 7.7 Hz); 8.19−8.10 (m, 1H); 8.05−7.96 (m, 2H); 7.85−7.73 (m, 1H); 7.65 (t, 1H); 7.57−7.48 (m, 1H); 7.45−7.35 (m, 1H).

Synthesis [Pd(pyqui-H)(OAc)(PPh$_3$)], 4

A mixture of [Pd_2(pyqui-H)$_2$(μ-OAc)$_2$] (149.4 mg, 0.20 mmol) and PPh_3 (80 mg, 0.3 mmol) are reacted in acetone (20 mL) was stirred at room temperature for 1 h. The solution was concentrated to small volume and the product was precipitated by the dropwise addition of diethyl ether. The precipitate was stirred for ca. 30 min, collected by vacuum filtration, and dried under vacuum to afford the product as a red solid (240.3 mg, 0.327 mmol, yield 82%). MP 128−130 °C (dec). Elemental Analysis, calculated for: $C_{34}H_{27}N_2O_2PPd$: C, 64.51; H, 4.30; N, 4.43%; found: 64.36; H, 4.53; N, 4.22%. ^{1}H NMR ($CDCl_3$) δ 8.73−8.69 (m, 1H); 8.57 (d, 1H, J = 8.9 Hz); 8.02 (dt, 1H, J = 7.7 Hz, J = 1.6 Hz); 7.96−7.88 (m, 7H); 7.53−7.39 (m, 11H); 7.25−7.20 (m, 1H); 7.13 (d, 1H, J = 6.0 Hz); 6.91 (d, 1H, J = 8.5 Hz); 1.45 (s, 3H). ^{1}H NMR (DMSO-d_6) δ 8.60 (br m, 1H, $H^{6'}$), 8.50 (d, J = 7.9 Hz, 1H), 8.29 (td, J = 7.7, 1.4 Hz, 1H, $H^{4'}$), 7.91 (d, J = 8.4 Hz, 1H), 7.84−7.70 (m) and 7.67−7.45 (m) (overlapping aromatic

Downloaded from pubs.acs.org/acsodf/article-pdf/doi/10.1021/acsomega.6c09421/6915267/acsomega.6c09421.pdf by guest on 15 November 2026

https://doi.org/10.1021/acsomega.6c09421
ACS Omega XXXX, XXX, XXX−XXX

resonances; 17H), 7.31 (app t, J = 7.5 Hz, 1H), 7.07 (d, J = 5.8 Hz, 1H, H^4), 6.90 (d, J = 8.0 Hz, 1H), 1.24 (s, 3H, CH_3 OAc). $^{31}P\{^1H\}$ NMR ($CDCl_3$) δ 41.42 (s, 1P). $^{31}P\{^1H\}$ NMR (DMSO-d_6): δ 40.60 (s, 1P). IR (Nujol), cm^{-1}: 1585 (broad).

Synthesis [Pd(pyqui-H)(Cl)(PPh_3)], 5

A mixture of [Pd_2(pyqui-H)$_2$(μ-Cl)$_2$] (85.5 mg, 0.12 mmol) and PPh_3 (64.6 mg, 0.24 mmol) in acetone (20 mL) was stirred at room temperature for 1 h. The solution was concentrated under reduced pressure to a small volume, and the product was precipitated by the dropwise addition of diethyl ether. The precipitate was stirred for ca. 30 min, collected by vacuum filtration, and dried under vacuum to afford the product as an orange solid (97.8 mg, 0.17 mmol, 71%). Mp 218−220 °C (dec). Elemental Analysis, calculated for: $C_{32}H_{24}ClN_2PPd$: C, 63.07; H, 3.97; Cl, 5.82; N, 4.60%; found: C, 62.92; H, 3.74; N, 4.87%. ^1H NMR ($CDCl_3$) δ 9.76 (d, 1H, $H^{6'}$, J = 5.5 Hz); 8.57 (d, 1H, $H^{3'}$, J = 7.9 Hz); 8.02 (td, 1H, $H^{4'}$, J = 5.5 Hz); 7.95 (d, 1H); 7.91−7.82 (m, 6H); 7.54, 7.38 (m, 11H); 7.23 (t, 1H, H^7, J = 7.5 Hz); 7.04 (d, 1H, $^4J_{P-H}$ = 5.8 Hz, H^4); 6.85 (d, 1H, H^6, J = 8.1 Hz). ^{13}C NMR ($CDCl_3$), selected signals: δ 122.2 ($C^{3'}$); 149.92 ($C^{6'}$); 144.7 (C^4); 164.8 (C^2); 162.2 ($C^{2'}$). $^{31}P\{^1H\}$ NMR ($CDCl_3$) δ 42.46 (s, 1P).

■ ASSOCIATED CONTENT

Supporting Information

The Supporting Information is available free of charge at https://pubs.acs.org/doi/10.1021/acsomega.6c09421.

Figures S1−S31: NMR spectra of complexes **1**−**5** (PDF)

■ AUTHOR INFORMATION

Corresponding Authors

Antonio Zucca − *Department of Chemical, Physical, Mathematical and Natural Sciences, University of Sassari, Sassari I-07100, Italy; Consorzio Interuniversitario Reattività Chimica e Catalisi (CIRCC), Bari 70126, Italy;* orcid.org/0000-0003-4423-9382; Email: zucca@uniss.it

Alessandra Scano − *Department of Surgical Sciences, University of Cagliari, Cagliari 09124, Italy;* Email: alessandra.scano77@unica.it

Authors

Bruna Canu − *Department of Chemical, Physical, Mathematical and Natural Sciences, University of Sassari, Sassari I-07100, Italy*

Giacomo Senzacqua − *Department of Chemical, Physical, Mathematical and Natural Sciences, University of Sassari, Sassari I-07100, Italy; Consorzio Interuniversitario Reattività Chimica e Catalisi (CIRCC), Bari 70126, Italy*

Sergio Stoccoro − *Department of Chemical, Physical, Mathematical and Natural Sciences, University of Sassari, Sassari I-07100, Italy; Consorzio Interuniversitario Reattività Chimica e Catalisi (CIRCC), Bari 70126, Italy*

Maria I. Pilo − *Department of Chemical, Physical, Mathematical and Natural Sciences, University of Sassari, Sassari I-07100, Italy*

Germano Orrù − *Department of Surgical Sciences, University of Cagliari, Cagliari 09124, Italy*

Diletta Raspizzu − *Department of Surgical Sciences, University of Cagliari, Cagliari 09124, Italy*

Complete contact information is available at: https://pubs.acs.org/10.1021/acsomega.6c09421

Notes

The authors declare no competing financial interest.

■ ACKNOWLEDGMENTS

This research was funded by the European Union − NextGenerationEU − Mission 4, Component 2, Investment 1.1. PRIN 2022 PNRR Project "Noble metal complexes with heterocyclic nitrogen ligands: application as antimicrobials" code MUR (Italian Ministry for University and Research) Grant No. P2022PZ8JE (CUP J53D23014830001). The authors thank Maria Orecchioni, Department of Medicine, Surgery, and Pharmacy, University of Sassari, for NMR spectra acquisition. The authors thank the University of Sassari for covering the open access publication charges under the CARE-CRUI Read and Publish agreement with the American Chemical Society (ACS).

■ REFERENCES

(1) Albrecht, M. Cyclometalation Using D-Block Transition Metals: Fundamental Aspects and Recent Trends. *Chem. Rev.* **2010**, *110* (2), 576−623.

(2) Omae, I. *Cyclometalation Reactions: five-Membered Ring Products as Universal Reagents*; Springer Japan: Tokyo, 2014. DOI:

(3) Albrecht, M.; Van Koten, G. Platinum Group Organometallics Based on "Pincer" Complexes: Sensors, Switches, and Catalysts. *Angew. Chem., Int. Ed.* **2001**, *40* (20), 3750−3781.

(4) Li, K.; Chen, Y.; Lu, W.; Zhu, N.; Che, C. A Cyclometalated Platinum(II) Complex with a Pendent Pyridyl Motif as Solid-State Luminescent Sensor for Acidic Vapors. *Chem. − Eur. J.* **2011**, *17* (15), 4109−4112.

(5) Yu, H.; Yu, B.; Song, Y.; Hai, P. Recent Advances of Cyclometalated Ir(III) Complexes for Optical Oxygen Sensing. *Inorg. Chim. Acta* **2023**, *550*, 121435.

(6) Kaswan, P.; Yadav, M.; Dhotre, S.; Minakshi, M.; Mehta, S. Applications of Luminescent Cyclometalated Metal Complexes as Sensors and Switches. *Synlett* **2025**, *36* (8), 921−943.

(7) Wu, F.-I.; Su, H.-J.; Shu, C.-F.; Luo, L.; Diau, W.-G.; Cheng, C.-H.; Duan, J.-P.; Lee, G.-H. Tuning the Emission and Morphology of Cyclometalated Iridium Complexes and Their Applications to Organic Light-Emitting Diodes. *J. Mater. Chem.* **2005**, *15* (10), 1035.

(8) Roberto, D.; Colombo, A.; Dragonetti, C.; Fagnani, F.; Cocchi, M.; Marinotto, D. A Novel Class of Cyclometalated Platinum(II) Complexes for Solution-Processable OLEDs. *Molecules* **2022**, *27* (16), 5171.

(9) Wang, D.; Chen, X.; Yang, H.; Zhong, D.; Liu, B.; Yang, X.; Yue, L.; Zhou, G.; Ma, M.; Wu, Z. The Synthesis of Cyclometalated Platinum(II) Complexes with Benzoaryl-Pyridines as C^N Ligands for Investigating Their Photophysical, Electrochemical and Electroluminescent Properties. *Dalton Trans.* **2020**, *49* (44), 15633−15645.

(10) Jurgens, S.; Kuhn, F. E.; Casini, A. Cyclometalated Complexes of Platinum and Gold with Biological Properties: State-of-the-Art and Future Perspectives. *Curr. Med. Chem.* **2018**, *25* (4), 437−461.

(11) Casini, A.; Kelter, G.; Gabbiani, C.; Cinellu, M. A.; Minghetti, G.; Fregona, D.; Fiebig, H.-H.; Messori, L. C. Antiproliferative Properties, Tumor Selectivity, and Molecular Mechanisms of Novel Gold(III) Compounds for Cancer Treatment: A Systematic Study. *JBIC, J. Biol. Inorg. Chem.* **2009**, *14* (7), 1139−1149.

(12) Carboni, S.; Zucca, A.; Stoccoro, S.; Maiore, L.; Arca, M.; Ortu, F.; Artner, C.; Keppler, B. K.; Meier-Menches, S. M.; Casini, A.; Cinellu, M. A. New Variations on the Theme of Gold(III) C^ N^ N Cyclometalated Complexes as Anticancer Agents: Synthesis and Biological Characterization. *Inorg. Chem.* **2018**, *57* (23), 14852−14865.

Downloaded from pubs.acs.org/acsodf/article-pdf/doi/10.1021/acsomega.6c09421/6915267/acsomega.6c09421.pdf by guest on 15 November 2026

(13) Cutillas, N.; Yellol, G. S.; De Haro, C.; Vicente, C.; Rodríguez, V.; Ruiz, J. Anticancer Cyclometalated Complexes of Platinum Group Metals and Gold. *Coord. Chem. Rev.* **2013**, *257* (19−20), 2784−2797.
(14) Amaya-Flórez, A.; R.-Galindo, J.; Sanchez-Yocue, E.; Ruiz-Martinez, A.; Serrano-García, J. S.; Romo-Pérez, A.; Cano-Sanchez, P.; Reyes-Marquez, V.; Le Lagadec, R.; Morales-Morales, D. Cyclometalated Complexes: Promising Metallodrugs in the Battle against Cancer. *RSC Med. Chem.* **2025**, *16* (11), 5125−5195.
(15) Fereidoonnezhad, M.; Shahsavari, H. R.; Abedanzadeh, S.; Behchenari, B.; Hossein-Abadi, M.; Faghih, Z.; Beyzavi, M. H. Cycloplatinated(II) Complexes Bearing 1,1′-Bis(Diphenylphosphino)-Ferrocene Ligand: Biological Evaluation and Molecular Docking Studies. *New J. Chem.* **2018**, *42* (4), 2385−2392.
(16) Chakraborty, P.; Oosterhuis, D.; Bonsignore, R.; Casini, A.; Olinga, P.; Scheffers, D. An Organogold Compound as Potential Antimicrobial Agent against Drug-Resistant Bacteria: Initial Mechanistic Insights. *ChemMedChem* **2021**, *16* (19), 3060−3070.
(17) Pintus, A.; Aragoni, M. C.; Cinellu, M. A.; Maiore, L.; Isaia, F.; Lippolis, V.; Orrù, G.; Tuveri, E.; Zucca, A.; Arca, M. [Au(Py b -H)(Mnt)]: A Novel Gold(III) 1,2-Dithiolene Cyclometalated Complex with Antimicrobial Activity (Py b -H = C-Deprotonated 2-Benzylpyridine; Mnt = 1,2-Dicyanoethene-1,2-Dithiolate). *J. Inorg. Biochem.* **2017**, *170*, 188−194.
(18) Zucca, A.; Canu, B.; Pilo, M. I.; Stoccoro, S.; Senzacqua, G.; Fais, S.; Pichiri, G.; Scano, A. Gold(III) Complexes with 2-(1-Ethylbenzyl)Pyridine as Promising Antimicrobial and Antitumor Agents. *Molecules* **2025**, *30* (7), 1611.
(19) Lu, L.; Liu, L.-J.; Chao, W.; Zhong, H.-J.; Wang, M.; Chen, X.-P.; Lu, J.-J.; Li, R.; Ma, D.-L.; Leung, C.-H. Identification of an Iridium(III) Complex with Anti-Bacterial and Anti-Cancer Activity. *Sci. Rep.* **2015**, *5* (1), 14544.
(20) Khan, E. Pyridine Derivatives as Biologically Active Precursors; Organics and Selected Coordination Complexes. *ChemistrySelect* **2021**, *6* (13), 3041−3064.
(21) Marinescu, M.; Popa, C. V. Pyridine Compounds with Antimicrobial and Antiviral Activities. *Int. J. Mol. Sci.* **2022**, *23* (10), 5659.
(22) Sahu, D.; Sreekanth, P. S. R.; Behera, P. K.; Pradhan, M. K.; Patnaik, A.; Salunkhe, S.; Cep, R. Advances in Synthesis, Medicinal Properties and Biomedical Applications of Pyridine Derivatives: A Comprehensive Review. *Eur. J. Med. Chem. Rep.* **2024**, *12* (September), 100210.
(23) *Comprehensive Coordination Chemistry II, Vol. 6, Transition Metal Groups 9−12*; Feton, D. E. eds., Elsevier: Amsterdam; 2003
(24) Zucca, A.; Pilo, M. I. Rollover Cyclometalation as a Valuable Tool for Regioselective C−H Bond Activation and Functionalization. *Molecules* **2021**, *26* (2), 328.
(25) Leist, M.; Kerner, C.; Ghoochany, L. T.; Farsadpour, S.; Fizia, A.; Neu, J. P.; Schön, F.; Sun, Y.; Oelkers, B.; Lang, J.; Menges, F.; Niedner-Schatteburg, G.; Salih, K. S. M.; Thiel, W. R. Roll-over Cyclometalation: A Versatile Tool to Enhance the Catalytic Activity of Transition Metal Complexes. *J. Organomet. Chem.* **2018**, *863*, 30−43.
(26) Butschke, B.; Schwarz, H. "Rollover" Cyclometalation − Early History, Recent Developments, Mechanistic Insights and Application Aspects. *Chem. Sci.* **2012**, *3* (2), 308−326.
(27) Maidich, L.; Dettori, G.; Stoccoro, S.; Cinellu, M. A.; Rourke, J. P.; Zucca, A. Electronic and Steric Effects in Rollover C−H Bond Activation. *Organometallics* **2015**, *34* (5), 817−828.
(28) Cocco, F.; Zucca, A.; Stoccoro, S.; Serratrice, M.; Guerri, A.; Cinellu, M. A. Synthesis and Characterization of Palladium(II) and Platinum(II) Adducts and Cyclometalated Complexes of 6,6′-Dimethoxy-2,2′-Bipyridine: $C(Sp^3)$−H and $C(Sp^2)$−H Bond Activations. *Organometallics* **2014**, *33* (13), 3414−3424.
(29) Maidich, L.; Pilo, M. I.; Rourke, J. P.; Clarkson, G. J.; Canu, P.; Stoccoro, S.; Zucca, A. Classical vs. Non-Classical Cyclometalated Pt(II) Complexes. *Molecules* **2022**, *27* (21), 7249.
(30) Zucca, A.; Maidich, L.; Pilo, M. I.; Pischedda, S.; Sedda, M.; Stoccoro, S. Pt(II) Derivatives with Rollover-Coordinated 6-Substituted 2,2′-Bipyridines: Ligands with Multiple Personalities. *Appl. Sci.* **2020**, *10* (19), 6665.
(31) Minghetti, G.; Stoccoro, S.; Cinellu, M. A.; Petretto, G. L.; Zucca, A. N,C "Rollover" Cyclometalated Platinum(II) Hydrides: Mono- and Polynuclear Derivatives. *Organometallics* **2008**, *27* (14), 3415−3421.
(32) Maidich, L.; Zuri, G.; Stoccoro, S.; Cinellu, M. A.; Masia, M.; Zucca, A. Mesoionic Complexes of Platinum(II) Derived from "Rollover" Cyclometalation: A Delicate Balance between Pt−C(sp 3) and Pt−C(sp 2) Bond Cleavage as a Result of Different Reaction Conditions. *Organometallics* **2013**, *32*, 438−448.
(33) Manca, L.; Senzacqua, G.; Stoccoro, S.; Zucca, A. Regioselective C(Sp2)-C(Sp3) Coupling Mediated by Classical and Rollover Cyclometalation. *Molecules* **2024**, *29* (3), 707.
(34) Babak, M. V.; Pfaffeneder-Kmen, M.; Meier-Menches, S. M.; Legina, S.; Theiner, S.; Licona, C.; Orvain, C.; Hejl, M.; Hanif, M. A.; Jakupec, M. A.; et al. Rollover Cyclometalated Bipyridine Platinum Complexes as Potent Anticancer Agents: Impact of the Ancillary Ligands on the Mode of Action. *Inorg. Chem.* **2018**, *57*, 2851−2864.
(35) Fereidoonnezhad, M.; Niazi, M.; Shahmohammadi Beni, M.; Mohammadi, S.; Faghih, Z.; Faghih, Z.; Shahsavari, H. R. Synthesis, Biological Evaluation, and Molecular Docking Studies on the DNA Binding Interactions of Platinum(II) Rollover Complexes Containing Phosphorus Donor Ligands. *ChemMedChem* **2017**, *12* (6), 456−465.
(36) Shahsavari, H. R.; Giménez, N.; Lalinde, E.; Moreno, M. T.; Fereidoonnezhad, M.; Babadi Aghakhanpour, R.; Khatami, M.; Kalantari, F.; Jamshidi, Z.; Mohammadpour, M. Heterobimetallic Pt^{II} -Au^{I} Complexes Comprising Unsymmetrical 1,1-Bis-(Diphenylphosphanyl)Methane Bridges: Synthesis, Photophysical, and Cytotoxic Studies. *Eur. J. Inorg. Chem.* **2019**, *2019* (10), 1360−1373.
(37) Murineddu, M.; Zucca, A.; Senzacqua, G.; Stoccoro, S.; Carraro, M.; Pilo, M. I.; Pichiri, G.; Orrù, G.; Scano, A. Platinum(II) Acetimino Cyclometalated Complexes Derived from Room Temperature Ammonia Activation. *Eur. J. Inorg. Chem.* **2024**, *27* (36), No. e202400491.
(38) Zucca, A.; Senzacqua, G.; Canu, A.; Ortu, F.; Stoccoro, S.; Pilo, M. I.; Orrù, G.; Pichiri, G.; Fais, S.; Scano, A. Pt(II) Rollover Cyclometalated Complexes Supported by 2,2'-Bipyridine N-Oxide: Synthesis, Characterisation and Biological Evaluation. *Organometallics* **2026**, *45*, 1698.
(39) Ahmed, S. K.; Hussein, S.; Qurbani, K.; Ibrahim, R. H.; Fareeq, A.; Mahmood, K. A.; Mohamed, M. G. Antimicrobial Resistance: Impacts, Challenges, and Future Prospects. *J. Med. Surg. Public Health* **2024**, *2*, 100081.
(40) Tang, K. W. K.; Millar, B. C.; Moore, J. E. Antimicrobial Resistance (AMR). *Br. J. Biomed. Sci.* **2023**, *80*, 11387.
(41) Murray, C. J. L.; Ikuta, K. S.; Sharara, F.; Swetschinski, L.; Robles Aguilar, G.; Gray, A.; Han, C.; Bisignano, C.; Rao, P.; Wool, E.; Johnson, S. C.; Browne, A. J.; Chipeta, M. G.; Fell, F.; Hackett, S.; Haines-Woodhouse, G.; Kashef Hamadani, B. H.; Kumaran, E. A. P.; McManigal, B.; Achalapong, S.; Agarwal, R.; Akech, S.; Albertson, S.; Amuasi, J.; Andrews, J.; Aravkin, A.; Ashley, E.; Babin, F.-X.; Bailey, F.; Baker, S.; Basnyat, B.; Bekker, A.; Bender, R.; Berkley, J. A.; Bethou, A.; Bielicki, J.; Boonkasidecha, S.; Bukosia, J.; Carvalheiro, C.; Castañeda-Orjuela, C.; Chansamouth, V.; Chaurasia, S.; Chiurchiù, S.; Chowdhury, F.; Clotaire Donatien, R.; Cook, A. J.; Cooper, B.; Cressey, T. R.; Criollo-Mora, E.; Cunningham, M.; Darboe, S.; Day, N. P. J.; De Luca, M.; Dokova, K.; Dramowski, A.; Dunachie, S. J.; Duong Bich, T.; Eckmanns, T.; Eibach, D.; Emami, A.; Feasey, N.; Fisher-Pearson, N.; Forrest, K.; Garcia, C.; Garrett, D.; Gastmeier, P.; Giref, A. Z.; Greer, R. C.; Gupta, V.; Haller, S.; Haselbeck, A.; Hay, S. I.; Holm, M.; Hopkins, S.; Hsia, Y.; Iregbu, K. C.; Jacobs, J.; Jarovsky, D.; Javanmardi, F.; Jenney, A. W. J.; Khorana, M.; Khusuwan, S.; Kissoon, N.; Kobeissi, E.; Kostyanev, T.; Krapp, F.; Krumkamp, R.; Kumar, A.; Kyu, H. H.; Lim, C.; Lim, K.; Limmathurotsakul, D.; Loftus, M. J.; Lunn, M.; Ma, J.; Manoharan, A.; Marks, F.; May, J.; Mayxay, M.; Mturi, N.; Munera-Huertas, T.; Musicha, P.; Musila, L. A.; Mussi-Pinhata, M. M.; Naidu, R. N.; Nakamura, T.; Nanavati, R.;

Downloaded from pubs.acs.org/acsodf/article-pdf/doi/10.1021/acsomega.6c09421/6915267/acsomega.6c09421.pdf by guest on 15 November 2026

Nangia, S.; Newton, P.; Ngoun, C.; Novotney, A.; Nwakanma, D.; Obiero, C. W.; Ochoa, T. J.; Olivas-Martinez, A.; Olliaro, P.; Ooko, E.; Ortiz-Brizuela, E.; Ounchanum, P.; Pak, G. D.; Paredes, J. L.; Peleg, A. Y.; Perrone, C.; Phe, T.; Phommasone, K.; Plakkal, N.; Ponce-de-Leon, A.; Raad, M.; Ramdin, T.; Rattanavong, S.; Riddell, A.; Roberts, T.; Robotham, J. V.; Roca, A.; Rosenthal, V. D.; Rudd, K. E.; Russell, N.; Sader, H. S.; Saengchan, W.; Schnall, J.; Scott, J. A. G.; Seekaew, S.; Sharland, M.; Shivamallappa, M.; Sifuentes-Osornio, J.; Simpson, A. J.; Steenkeste, N.; Stewardson, A. J.; Stoeva, T.; Tasak, N.; Thaiprakong, A.; Thwaites, G.; Tigoi, C.; Turner, C.; Turner, P.; Van Doorn, H. R.; Velaphi, S.; Vongpradith, A.; Vongsouvath, M.; Vu, H.; Walsh, T.; Walson, J. L.; Waner, S.; Wangrangsimakul, T.; Wannapinij, P.; Wozniak, T.; Young Sharma, T. E. M. W.; Yu, K. C.; Zheng, P.; Sartorius, B.; Lopez, A. D.; Stergachis, A.; Moore, C.; Dolecek, C.; Naghavi, M. Global Burden of Bacterial Antimicrobial Resistance in 2019: A Systematic Analysis. *Lancet* **2022**, *399* (10325), 629−655.

(42) Sati, H.; Carrara, E.; Savoldi, A.; Hansen, P.; Garlasco, J.; Campagnaro, E.; Boccia, S.; Castillo-Polo, J. A.; Magrini, E.; Garcia-Vello, P.; Wool, E.; Gigante, V.; Duffy, E.; Cassini, A.; Huttner, B.; Pardo, P. R.; Naghavi, M.; Mirzayev, F.; Zignol, M.; Cameron, A.; Tacconelli, E.; Aboderin, A.; Al Ghoribi, M.; Al-Salman, J.; Amir, A.; Apisarnthanarak, A.; Blaser, M.; El-Sharif, A.; Essack, S.; Harbarth, S.; Huang, X.; Kapoor, G.; Knight, G.; Muhwa, J. C.; Monnet, D. L.; Ousassa, T.; Sacsaquispe, R.; Severin, J.; Sugai, M.; Taneja, N.; Umubyeyi Nyaruhirira, A. The WHO Bacterial Priority Pathogens List 2024: A Prioritisation Study to Guide Research, Development, and Public Health Strategies against Antimicrobial Resistance. *Lancet Infect. Dis.* **2025**, *25* (9), 1033−1043.

(43) Nasiri Sovari, S.; Zobi, F. Recent Studies on the Antimicrobial Activity of Transition Metal Complexes of Groups 6−12. *Chemistry* **2020**, *2* (2), 418−452.

(44) Makuve, N.; Makuve, R. Metal Complexes as Antimicrobial, Antiviral and Antiparasitic Agents. *Br. J. Healthc. Med. Res.* **2025**, *12* (2), 200−212.

(45) Wang, C.; Wei, X.; Zhong, L.; Chan, C.-L.; Li, H.; Sun, H. Metal-Based Approaches for the Fight against Antimicrobial Resistance: Mechanisms, Opportunities, and Challenges. *J. Am. Chem. Soc.* **2025**, *147* (15), 12361−12380.

(46) Ming, L. Structure and Function of "Metalloantibiotics. *Med. Res. Rev.* **2003**, *23* (6), 697−762.

(47) Flemming, H.-C.; Wingender, J.; Szewzyk, U.; Steinberg, P.; Rice, S. A.; Kjelleberg, S. Biofilms: An Emergent Form of Bacterial Life. *Nat. Rev. Microbiol.* **2016**, *14* (9), 563−575.

(48) Giunta, D.; Solinas, M.; Canu, B.; Pilo, M. I.; Scano, A.; Orrù, G.; Fais, S.; Pichiri, G.; Zucca, A. Synthesis, Characterization, and Biological Evaluation of Noble Metal Complexes with 2-(1-Benzyl-1 H-1,2,3-triazol-4-yl)pyridine Ligand: An Interesting Class of Metallo-antimicrobial and -antitumor Agents. *ACS Omega* **2026**, *11* (2), 24597−24610.

(49) Zucca, A.; Murineddu, M.; Ortu, F.; Liu, Y.; Manca, G.; Orrù, G.; Scano, A.; Pilo, M. I. Pt(II) RolloverComplexes with Poor-Donor Bipyridines: Synthesis, Reactivity, and Preliminary Antimicrobial Evaluation. *ACS Omega* **2026**, *11*, 47011.

(50) Zucca, A.; Cordeschi, D.; Maidich, L.; Pilo, M. I.; Masolo, E.; Stoccoro, S.; Cinellu, M. A.; Galli, S. Rollover Cyclometalation with 2-(2′-Pyridyl)Quinoline. *Inorg. Chem.* **2013**, *52* (13), 7717−7731.

(51) Minghetti, G.; Doppiu, A.; Zucca, A.; Stoccoro, S.; Cinellu, M. A.; Manassero, M.; Sansoni, M. Palladium (II) and Platinum(II)-C(3)-Substituted 2,2′-Bipyridines. *Chem. Heterocycl. Compd.* **1999**, *35* (8), 992−1000.

(52) Zucca, A.; Cinellu, M. A.; Pinna, M. V.; Stoccoro, S.; Minghetti, G.; Manassero, M.; Sansoni, M. Cyclopalladation of 6-Substituted-2,2′-Bipyridines. Metalation of Unactivated Methyl Groups vs Aromatic C−H Activation. *Organometallics* **2000**, *19* (21), 4295−4304.

(53) Yu, J.; Lv, W.; Cheng, G. Palladium-Catalyzed Site-Selective C−H Arylation of 2,2′-Bipyridine-6-Carboxamides via a Rollover Cyclometalation Pathway. *Org. Lett.* **2018**, *20* (16), 4732−4735.

(54) Al-Afyouni, M. H.; Rohrabaugh, T. N.; Al-Afyouni, K. F.; Turro, C. New Ru(II) Photocages Operative with near-IR Light: New Platform for Drug Delivery in the PDT Window. *Chem. Sci.* **2018**, *9* (32), 6711−6720.

(55) Chan, K. H.-Y.; Chow, H.-S.; Wong, K. M.-C.; Yeung, M. C.-L.; Yam, V.-W.-W. Towards Thermochromic and Thermoresponsive Near-Infrared (NIR) Luminescent Molecular Materials through the Modulation of Inter- and/or Intramolecular Pt···Pt and $\pi-\pi$ Interactions. *Chem. Sci.* **2010**, *1* (4), 477.

(56) Fizia, A.; Gaffga, M.; Lang, J.; Sun, Y.; Niedner-Schatteburg, G.; Thiel, W. R. Cyclopalladation in the Periphery of a NHC Ligand as the Crucial Step in the Synthesis of Highly Active Suzuki−Miyaura Cross-Coupling Catalysts. *Chem. − Eur. J.* **2017**, *23* (58), 14563−14575.

(57) Bailey, W. D.; Phearman, A. S.; Luconi, L.; Rossin, A.; Yakhvarov, D. G.; D'accolti, L.; Flowers, S. E.; Kaminsky, W.; Kemp, R. A.; Giambastiani, G.; et al. Hydrogenolysis of Dinuclear PCN^{R} Ligated Pd^{II} μ-Hydroxides and Their Mononuclear Pd^{II} Hydroxide Analogues. *Chem. − Eur. J.* **2019**, *25* (42), 9920−9929.

(58) Petretto, G. L.; Zucca, A.; Stoccoro, S.; Cinellu, M. A.; Minghetti, G. Step by Step Palladium Mediated Syntheses of New 2-(Pyridin-2-Yl)-6-R-Nicotinic Acids and Esters. *J. Organomet. Chem.* **2010**, *695* (2), 256−259.

(59) Farsadpour, S.; Ghoochany, L. T.; Sun, Y.; Thiel, W. R. Small Substituents Make Large Differences: Aminopyrimidinyl Phosphanes Undergoing C−H Activation. *Eur. J. Inorg. Chem.* **2011**, *2011* (29), 4603−4609.

(60) Hackenberger, D.; Song, B.; Grünberg, M. F.; Farsadpour, S.; Menges, F.; Kelm, H.; Groß, C.; Wolff, T.; Niedner-Schatteburg, G.; Thiel, W. R.; Gooßen, L. J. Bimetallic Cu/Pd Catalysts with Bridging Aminopyrimidinyl Phosphines for Decarboxylative Cross-Coupling Reactions at Moderate Temperature. *ChemCatChem* **2015**, *7* (21), 3579−3588.

(61) Zucca, A.; Petretto, G. L.; Stoccoro, S.; Cinellu, M. A.; Manassero, M.; Manassero, C.; Minghetti, G. Cyclometalation of 2,2′-Bipyridine. Mono- and Dinuclear C,N Platinum(II) Derivatives. *Organometallics* **2009**, *28*, 2150−2159.

(62) Petretto, G. L.; Rourke, J. P.; Maidich, L.; Stoccoro, S.; Cinellu, M. A.; Minghetti, G.; Clarkson, G. J.; Zucca, A. Heterobimetallic Rollover Derivatives. *Organometallics* **2012**, *31* (8), 2971−2977.

(63) Minghetti, G.; Zucca, A.; Stoccoro, S.; Cinellu, M. A.; Manassero, M.; Sansoni, M. Six-Membered Cyclometallated Derivatives of Platinum(II) Derived from 2-Benzylpyridines. Crystal and Molecular Structure of [Pt(L)(Ph,P)Cl] (HL = 2-(l-Methylben ∼ l)Pyridine). *J. Organomet. Chem.* **1994**, *481*, 195−204.

(64) Hashemi Fath, R.; Hoseini, S. J. Covalently Cyclopalladium(II) Complex/Reduced-Graphene Oxide as the Effective Catalyst for the Suzuki−Miyaura Reaction at Room Temperature. *J. Organomet. Chem.* **2017**, *828*, 16−23.

Downloaded from pubs.acs.org/acsodf/article-pdf/doi/10.1021/acsomega.6c09421/6915267/acsomega.6c09421.pdf by guest on 15 November 2026

https://doi.org/10.1021/acsomega.6c09421
ACS Omega XXXX, XXX, XXX−XXX